Highly Conductive and Transparent PEDOT:PSS Films with a Fluorosurfactant for Stretchable and Flexible Transparent Electrodes

*Michael Vosgueritchian, Darren J. Lipomi, and Zhenan Bao**

Highly conductive and transparent poly-(3,4-ethylenedioxythiophene):poly(styrenesulfonic acid) (PEDOT:PSS) films, incorporating a fluorosurfactant as an additive, have been prepared for stretchable and transparent electrodes. The fluorosurfactant-treated PEDOT:PSS films show a 35% improvement in sheet resistance (R_s) compared to untreated films. In addition, the fluorosurfactant renders PEDOT:PSS solutions amenable for deposition on hydrophobic surfaces, including pre-deposited, annealed films of PEDOT:PSS (enabling the deposition of thick, highly conductive, multilayer films) and stretchable poly(dimethylsiloxane) (PDMS) substrates (enabling stretchable electronics). Four-layer PEDOT:PSS films have an R_s of 46 Ω per square with 82% transmittance (at 550 nm). These films, deposited on a pre-strained PDMS substrate and buckled, are shown to be reversibly stretchable, with no change to R_s, during the course of over 5000 cycles of 0 to 10% strain. Using the multilayer PEDOT:PSS films as anodes, indium tin oxide (ITO)-free organic photovoltaics are prepared and shown to have power conversion efficiencies comparable to that of devices with ITO as the anode. These results show that these highly conductive PEDOT:PSS films can not only be used as transparent electrodes in novel devices (where ITO cannot be used), such as stretchable OPVs, but also have the potential to replace ITO in conventional devices.

1. Introduction

Next-generation optoelectronic devices, such as solar cells, electronic paper, touch screens, and displays, based on conjugated polymers, small molecules, colloidal semiconductors, and carbon allotropes, require materials and processing techniques that are low-cost and compatible with deposition over large areas on plastic substrates.[1] The usefulness of these materials would be broadened by the ability to accommodate bending and tensile strain (flexibility and stretchability), which not only make them amenable to devices that require mechanical compliance, but also more durable. Solar cells and displays require at least one electrode material that must, additionally, be both highly conductive and transparent. Currently, indium tin oxide (ITO) is the material used as this transparent electrode (TE) due to its excellent optoelectronic properties, with a sheet resistance (R_s) on the order of 10 Ω per square (Ω $\square^{-1}$) at about 90% transparency (T).[2] However, ITO suffers from two major drawbacks that render it a non-ideal choice as a TE for next-generation devices: 1) the increasing price and scarcity of indium, which makes it difficult for its use in low-cost, large-area electronics and (2) the brittleness of ITO films, which render them unsuitable for applications that require stretchability or flexibility.[3] There are several emerging materials that have shown promise for the replacement of ITO films that have the potential for large-area coverage and some degree of mechanical compliance. These materials include carbon nanotubes (CNTs),[4,5] graphene,[6] metallic nanowires,[7,8] and conducting polymers.[9,10]

Carbon nanotubes possess several properties that make them good candidates as electrodes: high intrinsic conductivity, solution processability, durability, and the potential for production at low cost.[11] However, the large variations in tube types, such as diameters, lengths, and chirality, the difficulties in forming uniform films over large areas, and the large tube-to-tube junction resistance have prevented the adoption of CNTs as a TE by industry, though important research on dopants and methods of processing continues to improve CNT films.[12,13] Graphene, despite its relatively recent discovery in 2003, has almost matched, if not exceeded, CNTs in performance as a TE. Bae et al. demonstrated roll-to-roll transfer of 30-inch graphene films with a sheet resistance and transparency of 30 Ω $\square^{-1}$ at 90% T.[6] This process, however, requires chemical vapor deposition (CVD) growth of graphene on a copper foil, which must then be etched to transfer the graphene film to a flexible substrate and has to be repeated several times to achieve such a low sheet resistance. In contrast, solution-based methods of producing graphene are low-cost and directly compatible with flexible substrates; however, their sheet resistance is higher by an order of magnitude or more compared to CVD-grown films.[14,15] Metallic nanowires, in particular, films

M. Vosgueritchian, Dr. D. J. Lipomi, Prof. Z. Bao
Department of Chemical Engineering
Stanford University
381 North-South Mall, Stanford, CA 94305-5025, USA
E-mail: zbao@stanford.edu

DOI: 10.1002/adfm.201101775

of silver nanowires (AgNWs), have optical and electronic properties similar to that of ITO films with the added advantage of solution processability and flexibility.[8,16] The stability of these films, however, has been in question, and research is currently ongoing to determine methods to increase their lifetime and stability.[17]

Despite their discovery decades before the emerging nanomaterials described, conducting polymers have only been utilized commercially as TEs in niche applications, such as in inorganic electroluminescent lamps.[10] In particular, poly(3,4-ethylenedioxythiophene) (PEDOT) has been the most successful conducting polymer due to its high conductivity (when doped) and stability. The most common form of PEDOT is a formulation doped with poly(styrenesulfonic acid) (PSS). The negatively charged PSS allows PEDOT to be dispersed in an aqueous solution and serves as the counterion for the positively charged, oxidatively doped PEDOT.[18] Aqueous suspensions of PEDOT:PSS are commercially available (95–99% water) and allow for facile preparation of films with common coating methods, such as spin-coating. The conductivity of the resulting PEDOT:PSS film is highly dependent on the ratio of PEDOT to PSS and particle size of the PEDOT:PSS dispersions in water. Haraeus (formerly H. C. Starck) is a leading commercial manufacturer of PEDOT:PSS and has a variety of different grades available. The most conductive formulation (CLEVIOS PH 1000) has a reported conductivity of about 900 S cm^{-1} after the addition of 5% dimethylsulfoxide (DMSO).[19] The role of the DMSO is as a "secondary dopant," which improves PEDOT:PSS morphology and increases the conductivity of a PEDOT:PSS film by 2–3 orders of magnitude. Other inert, high-boiling polar compounds have also been used to increase the conductivity of PEDOT:PSS films, such as sorbitol, N-methylpyrrolidone, and diethylene glycol.[20,21] Despite numerous studies on the role of these compounds, the mechanism of the conductivity improvement in these films remains unclear. However, it is evident that these additives cause a rearrangement in the morphology of the films upon drying. This rearrangement may result in larger PEDOT grains or increased phase separation between the conducting PEDOT and the insulating PSS, leading to a better conducting network and can even change the work function of the film.[22,23] Other strategies have been used to improve the conductivity of PEDOT:PSS films including the use of a co-solvent system, zwitterionic surfactants, or exposing the films to dichloroacetic acid.[24–26] Kim et al. have used a solvent (ethylene glycol) and thermal post-treatment process on pre-deposited films to produce highly conductive PEDOT:PSS films, with an R_s of 65 Ω $\square^{-1}$ at 80% T, and have shown these films to be viable TE materials for ITO-free organic photovoltaics (OPVs).[27]

In this work, we report PEDOT:PSS films with a record R_s of 46 Ω $\square^{-1}$ at 82% T and 240 Ω $\square^{-1}$ at 97% T. The conductivity of the PEDOT:PSS film was improved using a combination of DMSO and the fluorosurfactant Zonyl-FS300 (Zonyl). In addition, the fluorosurfactant improved the wetting properties of the PEDOT:PSS solution, which enabled the facile deposition of highly conducting PEDOT:PSS films on a variety of hydrophobic substrates that would otherwise not be possible. These films were shown to be both stretchable and flexible when deposited on a buckled poly(dimethylsiloxane) (PDMS) substrate and capable of replacing ITO as the anode in devices such as organic photovoltaics (OPVs).

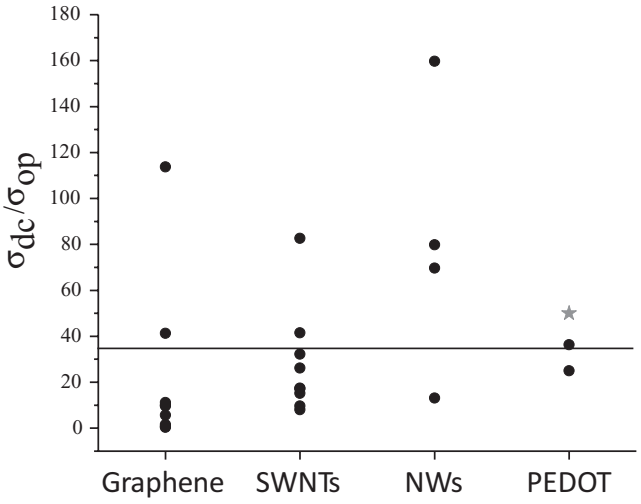

Figure 1. DC to optical conductivity ratios (σ_{dc}/σ_{op}) for emerging transparent electrodes (TEs). The star indicates the best results in this work. The solid black line at σ_{dc}/σ_{op} value of 35 indicates the minimum value needed for most TE applications. References for graphene from lowest to highest: [6,14,36–42]. References for SWNTs from lowest to highest: [5,43–50]. References for NWs from lowest to highest: [7,16,51,52]. References for PEDOT from lowest to highest: PH1000 control [27], doped PH1000 from this work [star].

2. Results and Discussion

2.1. Electrical Conductivity of Films

The following relationship can be used to relate the sheet resistance of a thin TE film to its transmittance:

$$T(\lambda) = \left(1 + \frac{188.5}{R_S}\frac{\sigma_{op}(\lambda)}{\sigma_{dc}}\right)^{-2}$$

where λ is the wavelength of light at which the transmittance is measured (typically 550 nm), and σ_{op} and σ_{dc} are the optical and direct current (DC) conductivities of the material, respectively.[28] Originally developed for thin metallic films, this relationship can be extended to alternative TEs as well. Using the ratio σ_{dc}/σ_{op} as a figure of merit, it is possible to quantitatively compare the different types of TEs. **Figure 1** shows some of the best σ_{dc}/σ_{op} values for TE films (over 80% T at 550 nm) of PEDOT, graphene, CNTs, and metallic NWs. It is generally agreed that TEs need to have σ_{dc}/σ_{op} of at least 35 for use in practical devices, which corresponds to an $R_s < 100$ with a $T > 90\%$. However, some applications such as in LCD displays require σ_{dc}/σ_{op} values of upwards of 50, whereas other applications such as touch screens require a less stringent σ_{dc}/σ_{op} value of about 10.[1]

In this work, typical values of σ_{dc}/σ_{op} achieved for PEDOT:PSS films were over 40, and the best films exhibited values of approximately 50 (depicted by the star in Figure 1), which is one of the best reported values for PEDOT:PSS films.

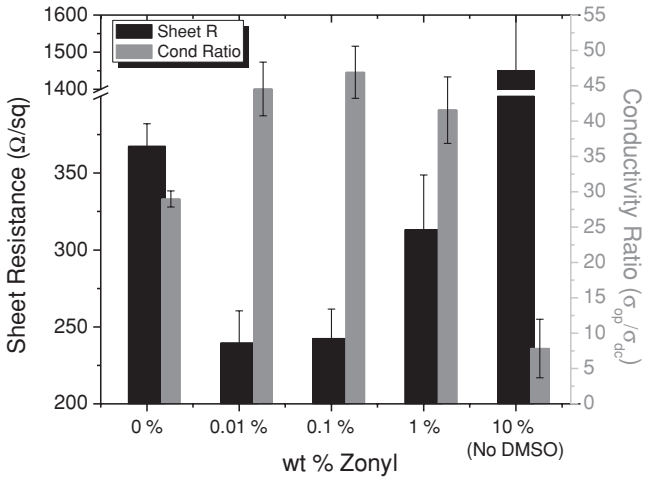

Figure 2. DC to optical conductivity ratios (σ_{dc}/σ_{op}) and sheet resistance (R_s) vs Zonyl concentration in wt% for four samples per condition across two batches. All samples were one layer and with 5% DMSO, except where noted.

We found that the conductivity of the PEDOT:PSS films were further enhanced by adding Zonyl, in addition to DMSO, to a PEDOT:PSS solution. Zonyl has been used with PEDOT previously to improve the wetting of PEDOT:PSS solutions but has not been investigated as an additive to enhance the PEDOT:PSS conductivity.[21,29] The sheet resistance of the purchased PEDOT:PSS without additives was over 10^5 Ω □$^{-1}$ at 97% *T* (at 550 nm). With the addition of 5 wt% DMSO, the sheet resistance decreased to 370 Ω □$^{-1}$ at 97% *T*. With the addition of small amounts of Zonyl (0.01 wt% to 0.1 wt%), the conductivity further increased by 35% to 240 Ω □$^{-1}$ with no change in *T* (~97% at 550 nm for one layer films). In fact, even without DMSO, Zonyl improved the conductivity of the PEDOT:PSS films by two orders of magnitude (see the Supporting Information), but the best results were obtained using both DMSO and Zonyl as additives. **Figure 2** shows the R_s and σ_{dc}/σ_{op} of the PEDOT films as a function of Zonyl concentration.

We attributed this improvement in conductivity to an increase in phase separation between the PEDOT and PSS chains, which allowed the formation of more conductive PEDOT channels. **Figure 3** shows high-resolution atomic force microscopy (AFM) height images that reflect the morphological changes in the films as the concentration of Zonyl was increased. As can be seen, with increasing Zonyl concentrations, the separation of the PEDOT and PSS increased, and consequently, better conductive pathways formed in the film. Figure 3a shows the height AFM image of the PEDOT:PSS film with no Zonyl. Small grains of 20–30 nm were observed on the surface, which is consistent with the previously reported structure of PEDOT:PSS films as PEDOT-rich grains surrounded by thin PSS layers.[22] The corresponding phase images of this films (**Figure 4**) corroborated the height image with the bright regions corresponding to PEDOT-rich areas and the dark regions corresponding to PSS-rich areas. It has been shown that for polymer systems, a lower phase angle corresponds to a softer material (darker regions).[30] Because PSS is hygroscopic, it is expected to swell and be relatively soft compared to the more rigid conjugated polymer, PEDOT.[21] Once Zonyl is introduced to the film, the grains become elongated and start to form longer connected networks of PEDOT-rich areas as the PEDOT and PSS regions phase segregate. This mechanism has been observed several times in association with improved conductivity in PEDOT:PSS films. Xia et al. used both a cosolvent system and zwitterionic surfactants to induce phase segregation in PEDOT:PSS films.[24,25] Crispin et al. performed detailed studies on the effect of adding diethyl glycol (DEG) to PEDOT:PSS solutions.[21] The authors discovered that DEG induces phase segregation in the film, which was confirmed using tapping AFM images. Finally, Kim et al. used a thermal post-treatment process to induce phase segregation in PEDOT:PSS films after the films were deposited.[27] In all of these cases, AFM images showed that the PEDOT-rich grains were elongated and formed more interconnected networks, which was what we have observed in our system. Figure 3c and d (with corresponding phase images in Figure 4c and d) show the increase in phase separation as the Zonyl concentration was increased to 1 wt% and

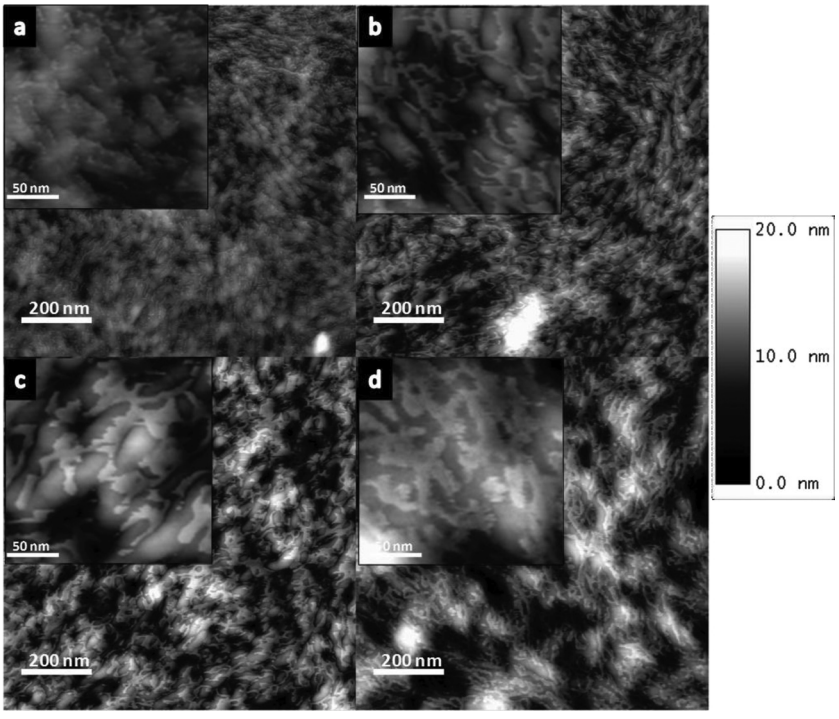

Figure 3. Topography (height) images of PEDOT:PSS films obtained with tapping-mode AFM. All images have a size of 1 μm × 1 μm and a height scale of 20 nm. The insets are a 3× zoom of the original image. a) 0 wt% Zonyl b) 0.1 wt% Zonyl c) 1 wt% Zonyl d) 10 wt% Zonyl.

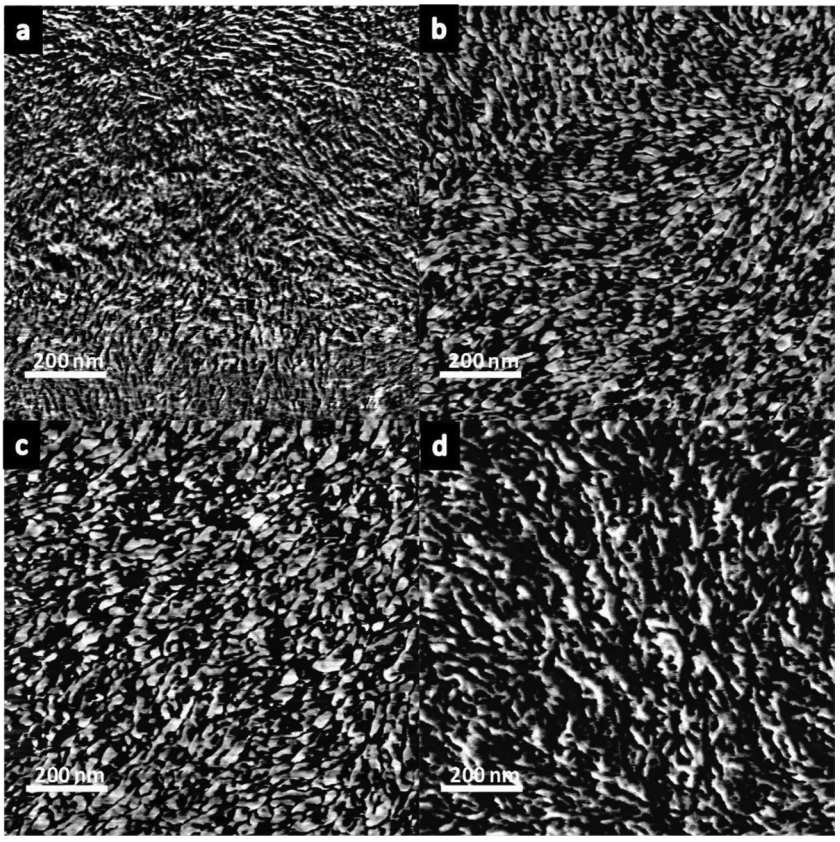

Figure 4. Corresponding phase images of PEDOT:PSS films of the topography images shown in Figure 3 obtained with tapping-mode AFM. All images have a size of 1 μm × 1 μm. a) 0 wt% Zonyl b) 0.1 wt% Zonyl c) 1 wt% Zonyl d) 10 wt% Zonyl.

10 wt%, respectively. However, because Zonyl is an insulating material and remains in the film, it begins to interfere with the conductive PEDOT pathways at high concentrations. As a result, the most conductive films were formed with Zonyl at about 0.01–0.1 wt%.

2.2. Multilayer PEDOT:PSS films

As mentioned previously, the addition of Zonyl to a PEDOT:PSS solution increases its wettablity on hydrophobic surfaces significantly, which is due to the amphiphilic nature of the Zonyl molecule. **Scheme 1** shows the chemical structure of Zonyl and PEDOT:PSS. Zonyl is composed of both a hydrophobic (fluorinated) and hydrophilic (ethylene glycol) segment enabling it to interact with the corresponding parts in PEDOT:PSS and makes the aqueous solution amenable to deposition on any substrate. This property enables the deposition of PEDOT:PSS films on substrates and films that are usually dewetted by aqueous solutions. In fact, an annealed PEDOT:PSS film is hydrophobic due to the PSS regions, which prohibits the formation of multilayer PEDOT:PSS films to reduce the sheet resistance. As a result, only very thin films, typically less than 100 nm, can be formed via spin-coating of normal PEDOT:PSS solutions. However, with the addition of Zonyl, multilayer films can be formed to produce highly conductive PEDOT:PSS layers.[31] Here, we used a layer-by-layer spin-coating process to form multilayer PEDOT:PSS films. **Figure 5** shows the transparency and the sheet resistance as a function of the number of layers for PEDOT:PSS films with 0.1 wt% Zonyl. Each layer was spun coat at 2000 rpm, the slowest speed possible to produce a uniform film across the substrates (2 cm × 2.5 cm). The transparency (at 550 nm) decreased linearly at approximately 4.5% loss of T per layer. The R_s initially decreased significantly per layer and then began to level off as it started to reach the bulk R_s. This

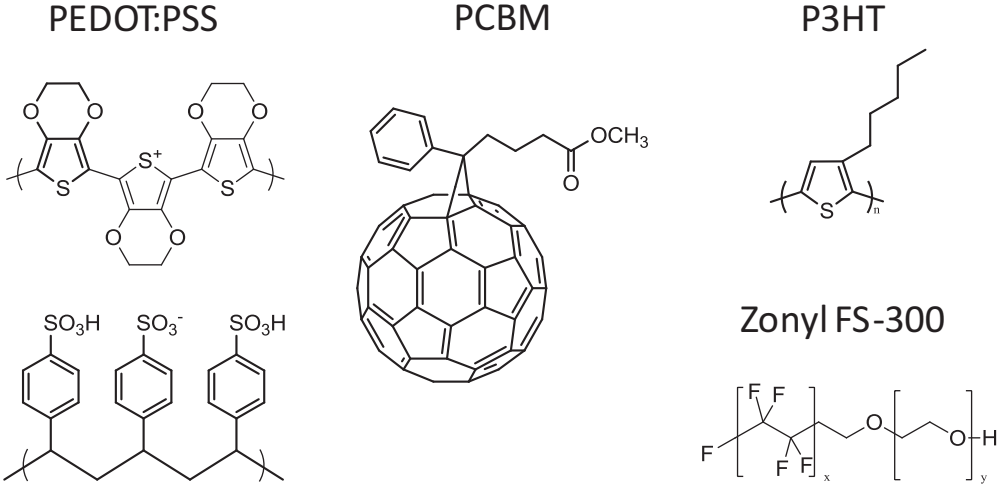

Scheme 1. Chemical structures of PEDOT:PSS, PCBM, P3HT, and Zonyl FS-300.

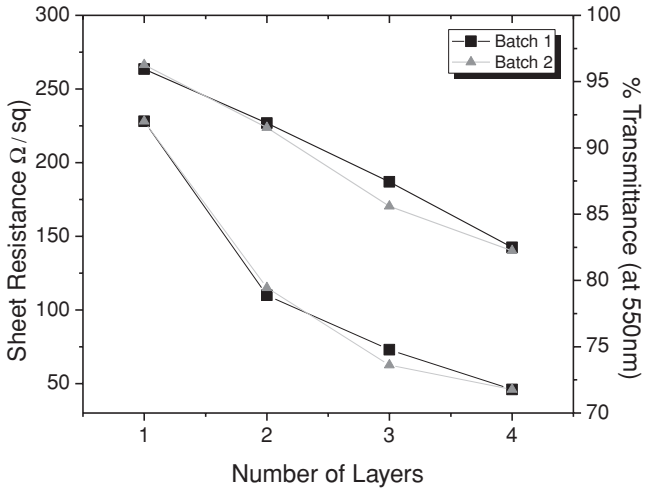

Figure 5. Number of PEDOT:PSS layers in a film versus sheet resistance (R_s) and transmittance (T) at 550 nm for two separate batches.

result is similar to what has been observed for thin metallic films.[32] At four layers, the film exhibited a sheet resistance of 46 Ω $\square^{-1}$ with a transmittance of 82% T (at 550 nm). With further improvements to commercially available PEDOT:PSS formulations, it could be possible to obtain or perhaps exceed the performance of ITO using this multilayer deposition method. In addition, combining our pre-processing technique with the post-processing methods described earlier might also present further improvements to the conductivity of PEDOT:PSS films.

2.3. PEDOT:PSS Films on Stretchable Substrates

We have recently demonstrated stretchable OPVs using PEDOT:PSS as the transparent electrode.[33] For such applications, it is not possible to use ITO because it is brittle and not compatible with plastic and flexible substrates. One of the major challenges using PEDOT:PSS on such substrates is its poor wetting, which prohibits the formation of a uniform film. However, using Zonyl doped solutions, it was possible to form uniform and reproducible films on stretchable PDMS substrates. Furthermore, our formulation rendered the PEDOT:PSS solution wettable on all hydrophobic surfaces we have tried, such as organic semiconductors or carbon nanotube films. (The more hydrophobic the film the larger amount of Zonyl was needed to wet the film properly to form uniform thin films.) By spin-coating the PEDOT:PSS on a pre-strained PDMS substrate and releasing the pre-strain, we were able to form buckles, or waves, which converted tensile strain of the film into bending strains of the buckles. A four-layer film with 1 wt% Zonyl was used for the stretching tests. The sheet resistance of the film when fully relaxed (buckled) was 150 Ω $\square^{-1}$ and the film was pre-strained to 15%. **Figure 6**a plots R_s as a function of 1, 10, 100, 1000, and 5000 cycles of stretching from 0 to 10%. As can be seen, the sheet resistance remained constant even after 5000 stretching cycles. The increase in the sheet resistance during the stretching test was completely due to the

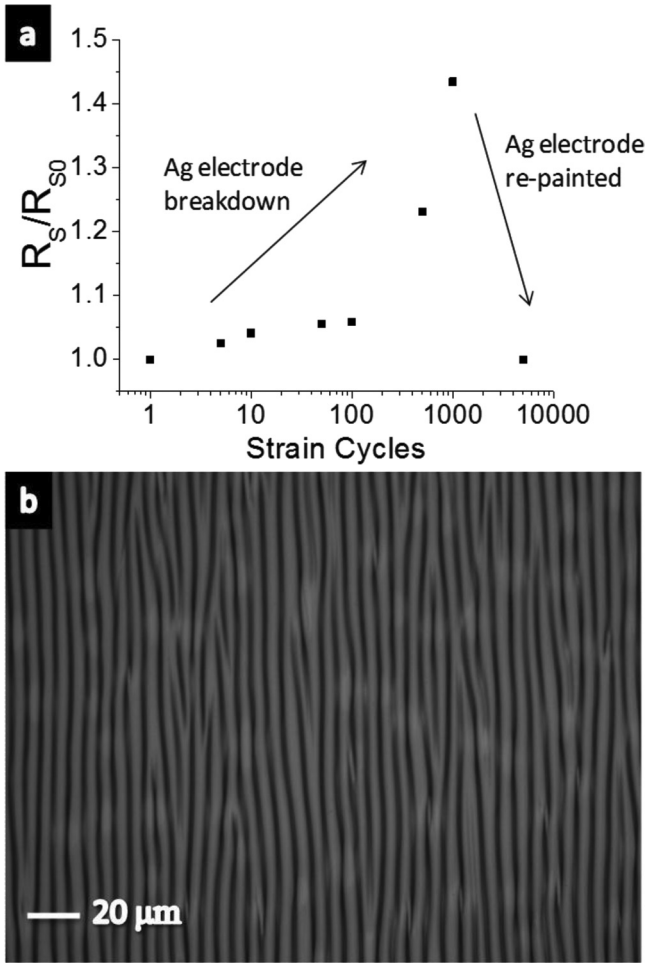

Figure 6. a) Normalized sheet resistance versus stretching cycles with 10% strain for 4-Layer, buckled PEDOT:PSS film with 1 wt% Zonyl. Original sheet resistance of the film was 150 Ω $\square^{-1}$. The increase in sheet resistance was due to the breakdown of the silver electrodes that were connected to the copper wires used for resistance measurements. After 5000 cycles the electrodes were repainted and the sheet resistance was identical to the original value. b) Optical microscopy image of the buckled PEDOT:PSS film (0% strain).

breakdown of the silver paint electrodes. After 5000 cycles the electrodes were repainted and the R_s returned to the original value of 150 Ω $\square^{-1}$. Figure 6b shows an optical microscopy image of the buckled films after releasing the strain. The buckles were approximately 5–6 μm apart. Furthermore, preliminary evidence suggests that the presence of Zonyl intrinsically improves the ability of PEDOT:PSS films to withstand strain without adversely effecting its electrical properties.[34]

2.4. OPVs using highly conductive PEDOT:PSS

The sheet resistance of the transparent electrodes plays a critical role in the power conversion efficiency (PCE) of photovoltaics. High values of R_s in transparent electrodes manifest in high series resistance, which has the effect of reducing the fill factor (FF), and thus the PCE. The effect is pronounced for

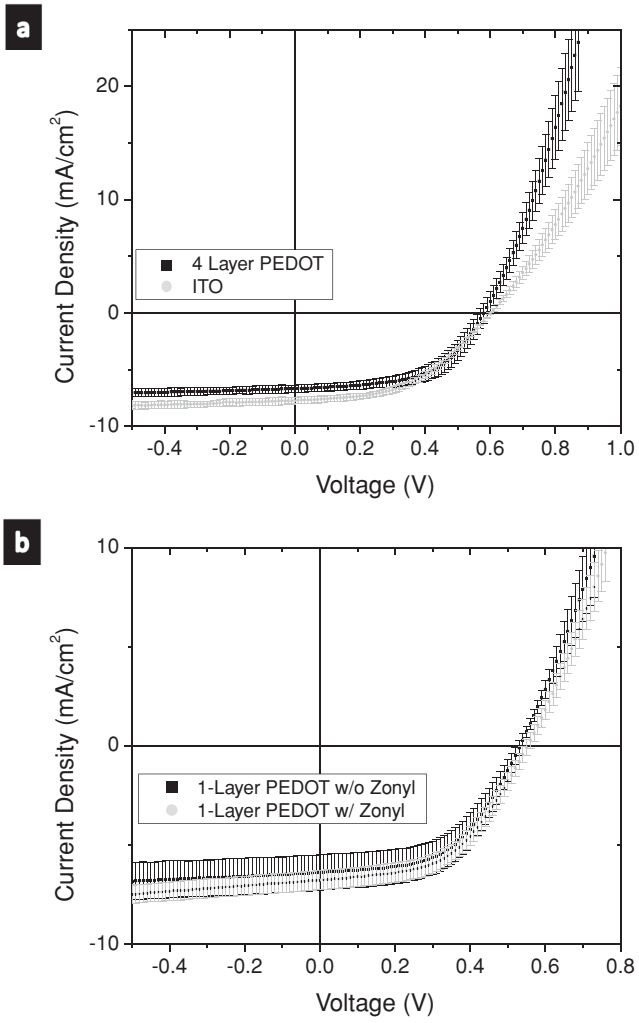

Figure 7. *J–V* characteristics of OPVs made with a P3HT:PCBM bulk heterojunction structure. a) Comparison between four-layer PEDOT:PSS film and ITO + AL4083 as the anodes. b) Comparison between one-layer PEDOT:PSS film with and without Zonyl as the anodes.

large area devices.[35] As a result, alternative electrodes must have similar performance to ITO (high conductivity and transparency). Despite the continuing improvement of PEDOT:PSS films by manufacturers, thick and highly conductive layers of PEDOT:PSS are needed to make the performance of these films comparable to that of ITO. As described earlier, our multilayer PEDOT:PSS films doped with DMSO and Zonyl can form highly conductive and transparent electrodes with values approaching that of ITO. ITO-free OPV devices were fabricated with these films by using a blend of P3HT and PCBM as the active layer. **Figure 7** shows the current density–voltage (*J–V*) curves for both the ITO free device and an ITO device, coated with PEDOT:PSS (CLEVIOS™ AL 4083, which smoothens the ITO and facilitates the extraction of holes), as a control. The ITO/AL 4083 control anode had an R_s of about 15 Ω □$^{-1}$. As can be seen, the performance of the OPVs fabricated with PEDOT:PSS as the anode was similar to the conventional ITO OPVs. While the ITO-free device exhibited higher open-circuit voltage (V_{OC}) and FF, the ITO control produced a greater overall PCE because of a greater short-circuit current density (J_{SC}). To compare the effect of the Zonyl on the PEDOT in OPV devices, one layer PEDOT devices were fabricated: one with no Zonyl and one with 0.1 wt% Zonyl. The device with Zonyl doped PEDOT showed better PV performance, which was attributed to the lower R_s of the film. The PV parameters, including J_{SC}, V_{OC}, FF, and PCE, are shown in **Table 1**.

3. Conclusions

In summary, we have prepared highly conductive and transparent PEDOT:PSS films with the use of the fluorosurfactant Zonyl as an additive to both improve the conductivity of the film and make it amenable for multilayer deposition on conventional and stretchable substrates. One layer films with Zonyl had an R_s of 240 Ω □$^{-1}$ at 97% *T* (at 550 nm), which was 35% better than films without Zonyl. Multilayer deposition could be used to produce films with R_s of 46 Ω □$^{-1}$ at 82% *T* (at 550 nm). Stretchable and flexible electrodes were made on prestrained PDMS substrates that were able to withstand over 5000 stretching cycles of 10% strain with no change in R_s. Bulk heterojunction OPV devices based on a blend of P3HT:PCBM were made using multilayer PEDOT:PSS films as the electrode. These OPVs performed comparably to conventional devices using ITO. The results indicate that the highly conductive PEDOT:PSS films can be used as transparent electrodes in novel devices, such as stretchable OPVs, in addition to replacing ITO in conventional devices.

4. Experimental Section

Materials: PEDOT:PSS solutions (CLEVIOS PH 1000 and CLEVIOS AL 4083) were purchased from Heraeus. The solid content of the PH 1000 solution was 1–1.3% and had a PEDOT to PSS ratio of 1:2.5 by weight. Zonyl FS-300 (Zonyl), DMSO, *ortho*-dichlorobenzene (*o*-DCB), poly(3-hexylthiophene) (P3HT, regioregular, >90% head-to-tail

Table 1. Photovoltaic parameters for OPVs made with four-layer and one-layer PEDOT:PSS films with Zonyl, one-layer PEDOT:PSS film without Zonyl, and ITO + AL4083 as the anodes.

Anode	Jsc [mA cm^{-2}]	Voc [mV]	FF	PCE [%]	Device Area [cm^2]	# of Devices
ITO + AL4083	7.75 ± 0.28	603 ± 5	0.475 ± 0.021	2.22 ± 0.11	0.087 ± 0.014	4
4-Layer PEDOT w/Zonyl	6.69 ± 0.35	580 ± 19	0.555 ± 0.038	2.16 ± 0.29	0.070 ± 0.025	10
1-Layer PEDOT w/Zonyl	6.77 ± 0.50	553 ± 12	0.510 ± 0.025	1.91 ± 0.18	0.048 ± 0.012	11
1-Layer PEDOT w/o Zonyl	6.37 ± 0.23	532 ± 10	0.532 ± 0.029	1.81 ± 0.17	0.045 ± 0.008	12

regiospecificity), [6,6]-phenyl C_{61} butyric acid methyl ester (PCBM, >99%), and eutectic gallium-indium (EGaIn, ≥99.99%) were purchased from Sigma–Aldrich and used as received. The PDMS was prepared by puddle-casting a mixed and degassed PDMS prepolymer (Dow Corning Sylgard 184, with a ratio of base to crosslinker of 10:1 by mass) against the polished surface of a silicon wafer. It was then cured at 60 °C for 2 h with a thickness of 200–500 μm and cut into desired sizes.

PEDOT:PSS Solution Formation and Film: The PEDOT:PSS was filtered through a syringe filter (0.45 μm pore size) to remove any large particles. Where noted, 5% by weight DMSO and different amounts of Zonyl were added to the PEDOT:PSS solution. The solution was placed on a shaker for at least one hour to ensure good mixing before spin-coating. The solutions were spun coat on clean substrates (glass or PDMS) at 2000 rpm for 60 s. They were then placed on a hot plate in ambient air for 5 min at 120 °C to dry. For multilayer films, the process was repeated after the films were dried.

Characterization of PEDOT:PSS Films: AFM images were taken using tapping mode (light tapping regime) using a Multimode AFM (Veeco). The R_s was measured using the four-point van der Pauw method with collinear probes (0.5 cm spacing) connected to a Keithley 2400 Sourcemeter. Optical microscopy images of the films were taken using a Leica DM4000M microscope under bright-field illumination. Optical transmission measurements were performed on Cary 6000i spectrophotometer from 250 to 1250 nm. Reported transmittances (T) are at 550 nm. Complete spectra are shown in Supporting Information. Stretching cycles were performed on an in-house stretching station with films on the PDMS substrate (see the Supporting Information). Silver paint electrodes were painted on two ends of the substrate (1 cm × 2 cm) and copper wire was pressed down on top to pin each end of the substrate. The copper wires were connected to an Agilent E4980A LCR meter to measure 2-point resistance during the stretching cycles.

Fabrication and Characterization of OPVs: The active layer solution was prepared with a 1:1 solution of P3HT:PCBM in *o*-DCB (30 mg mL^{-1} total). This solution was spun coat at 700 rpm for 1 min and 2000 rpm for 1 min on the desired substrate (PEDOT:PSS films or ITO). After spin-coating, the substrates were transferred to a nitrogen glovebox and annealed on a hotplate at 150 °C for 30 min; after annealing, the hotplate was turned off and the substrate was allowed to cool gradually for 30 min. The substrates were then removed from the glovebox and EGaIn was deposited on top for the top electrode. Copper wires were placed in each drop of EGaIn and secured to the edge of the substrate with tape. The devices were immediately returned to the glovebox (total time in the ambient atmosphere was <10 min). The areas of the devices were determined by integrating the area of contact between the EGaIn and the P3HT:PCBM from an optical micrograph. Typical device areas were ~0.05 cm^2. The photovoltaic properties were measured using a Newport solar simulator with a 100 mW cm^{-2} flux that approximated the solar spectrum under AM 1.5G conditions. We measured the current density vs. voltage in the dark and under illumination using a Keithley 2400 Sourcemeter and collected the data electronically using a custom LabView script.

Supporting Information

Supporting Information is available from the Wiley Online Library or from the author.

Acknowledgements

The authors would like to thank the Global Climate and Energy Project (GCEP) at Stanford University for funding this project. D.J.L. was supported by a postdoctoral fellowship from the U. S. Intelligence Community.

Received: August 1, 2011
Revised: October 3, 2011
Published online: November 25, 2011

[1] D. S. Hecht, L. Hu, G. Irvin, *Adv. Mater.* **2011**, *23*, 1482.
[2] R. B. H. Tahar, T. Ban, Y. Ohya, Y. Takahashi, *J. Appl. Phys.* **1998**, *83*, 2631.
[3] D. R. Cairns, R. P. Witteli, D. K. Sparacin, S. M. Sachsman, D. C. Paine, G. P. Crawford, R. R. Newton, *Appl. Phys. Lett.* **2000**, *76*, 1425.
[4] S. L. Hellstrom, H. W. Lee, Z. Bao, *ACS Nano* **2009**, *3*, 1423.
[5] C. Feng, K. Liu, J.-S. Wu, L. Liu, J.-S. Cheng, Y. Zhang, Y. Sun, Q. Li, S. Fan, K. Jiang, *Adv. Funct. Mater.* **2010**, *20*, 885.
[6] S. Bae, H. Kim, Y. Lee, X. Xu, J.-S. Park, Y. Zheng, J. Balakrishnan, T. Lei, H. Ri Kim, Y. I. Song, Y.-J. Kim, K. S. Kim, B. Ozyilmaz, J.-H. Ahn, B. H. Hong, S. Iijima, *Nat. Nanotechnol.* **2010**, *5*, 574.
[7] H. Wu, L. Hu, M. W. Rowell, D. Kong, J. J. Cha, J. R. McDonough, J. Zhu, Y. Yang, M. D. McGehee, Y. Cui, *Nano Lett.* **2010**, *10*, 4242.
[8] J.-Y. Lee, S. T. Connor, Y. Cui, P. Peumans, *Nano Lett.* **2008**, *8*, 689.
[9] S. Kirchmeyer, K. Reuter, *J. Mater. Sci.* **2005**, *15*, 2077.
[10] G. Wegner, *Angew. Chem., Int. Ed.* **1981**, *20*, 361.
[11] L. Hu, D. S. Hecht, G. Gruner, *Chem. Rev.* **2010**, *110*, 5790.
[12] M. S. Arnold, A. A. Green, J. F. Hulvat, S. I. Stupp, M. C. Hersam, *Nat. Nanotechnol.* **2006**, *1*, 60.
[13] R. K. Jackson, A. Munro, K. Nebesny, N. Armstrong, S. Graham, *ACS Nano* **2010**, *4*, 1377.
[14] U. Khan, A. O'Neill, M. Lotya, S. De, J. N. Coleman, *Small* **2010**, *6*, 864.
[15] F. Li, Y. Bao, J. Chai, Q. Zhang, D. Han, L. Niu, *Langmuir* **2010**, *26*, 12314.
[16] L. Hu, H. S. Kim, J.-Y. Lee, P. Peumans, Y. Cui, *ACS Nano* **2010**, *4*, 2955.
[17] B. Stahlmecke, F. J. M. z. Heringdorf, L. I. Chelaru, M. H.-v. Hoegen, G. Dumpich, K. R. Roos, *Appl. Phys. Lett.* **2006**, *88*, 053122.
[18] A. G. MacDiarmid, *Curr. Appl. Phys.* **2001**, *1*, 269.
[19] Provided by Clevios PH1000 maker, Haraeus: http://www.clevios.com/index.php?page_id = 3671.
[20] A. M. Nardes, M. Kemerink, M. M. de Kok, E. Vinken, K. Maturova, R. A. J. Janssen, *Org. Electron.* **2008**, *9*, 727.
[21] X. Crispin, F. L. E. Jakobsson, A. Crispin, P. C. M. Grim, P. Andersson, A. Volodin, C. van Haesendonck, M. Van der Auweraer, W. R. Salaneck, M. Berggren, *Chem. Mater.* **2006**, *18*, 4354.
[22] A. M. Nardes, *On the Conductivity of PEDOT:PSS Films*, PhD Thesis, Technische Universiteit Eindhoven, The Netherlands **2007**.
[23] M.-R. Choi, T.-H. Han, K.-G. Lim, S.-H. Woo, D. H. Huh, T.-W. Lee, *Angew. Chem. Int. Ed.* **2011**, *50*, 6274.
[24] Y. Xia, J. Ouyang, *J. Mater. Sci.* **2011**, *21*, 4927.
[25] Y. Xia, H. Zhang, J. Ouyang, *J. Mater. Sci.* **2011**, *20*, 9740.
[26] J. E. Yoo, K. S. Lee, A. Garcia, J. Tarver, E. D. Gomez, K. Baldwin, Y. Sun, H. Meng, T.-Q. Nguyen, Y.-L. Loo, *Proc. Natl. Acad. Sci. USA* **2010**, *107*, 5712.
[27] Y. H. Kim, C. Sachse, M. L. Machala, C. May, L. Müller-Meskamp, K. Leo, *Adv. Funct. Mater.* **2011**, *21*, 1009.
[28] M. Dressel, G. Gruner, *Electrodynamics of Solids: Optical Properties of Electrons in Matter*, Cambridge University Press, New York, USA **2003**.
[29] M. Bolognesi, A. Sanchez-Diaz, J. Ajuria, R. Pacios, E. Palomares, *Phys. Chem. Chem. Phys.* **2011**, *13*, 6105.
[30] Y. Wang, R. Song, Y. Li, J. Shen, *Surf. Sci* **2003**, *530*, 136.
[31] M. M. Voigt, R. C. I. Mackenzie, C. P. Yau, P. Atienzar, J. Dane, P. E. Keivanidis, D. D. C. Bradley, J. Nelson, *Sol. Energy Mater. Sol. Cells* **2011**, *95*, 731.
[32] J. Hautcoeur, X. Castel, F. Colombel, R. Benzerga, M. Himdi, G. Legeay, E. Motta-Cruz, *Thin Solid Films* **2011**, *519*, 3851.
[33] D. J. Lipomi, B. C. K. Tee, M. Vosgueritchian, Z. Bao, *Adv. Mater.* **2011**, *23*, 1771.
[34] D. J. Lipomi, J. A. Lee, M. Vosgueritchian, B. C.-K. Tee, J. A. Bolander, Z. Bao, unpublished.
[35] Y. Jun-Seok, Y. Jin-Mun, K. Seok-Soon, K. Dong-Yu, K. Junkyung, S.-I. Na, *Semicond. Sci. Technol.* **2011**, *26*, 034010.

[36] P. Blake, P. D. Brimicombe, R. R. Nair, T. J. Booth, D. Jiang, F. Schedin, L. A. Ponomarenko, S. V. Morozov, H. F. Gleeson, E. W. Hill, A. K. Geim, K. S. Novoselov, *Nano Lett.* **2008**, *8*, 1704.
[37] H. A. Becerril, J. Mao, Z. Liu, R. M. Stoltenberg, Z. Bao, Y. Chen, *ACS Nano* **2008**, *2*, 463.
[38] Y. Lee, S. Bae, H. Jang, S. Jang, S.-E. Zhu, S. H. Sim, Y. I. Song, B. H. Hong, J.-H. Ahn, *Nano Lett.* **2010**, *10*, 490.
[39] S. Biswas, L. T. Drzal, *Nano Lett.* **2008**, *9*, 167.
[40] X. Li, Y. Zhu, W. Cai, M. Borysiak, B. Han, D. Chen, R. D. Piner, L. Colombo, R. S. Ruoff, *Nano Lett.* **2009**, *9*, 4359.
[41] J.-H. Chen, C. Jang, S. Xiao, M. Ishigami, M. S. Fuhrer, *Nat. Nanotechnol.* **2008**, *3*, 206.
[42] F. Gunes, H.-J. Shin, C. Biswas, G. H. Han, E. S. Kim, S. J. Chae, J.-Y. Choi, Y. H. Lee, *ACS Nano* **2010**, *4*, 4595.
[43] A. A. Green, M. C. Hersam, *Nano Lett.* **2008**, *8*, 1417.
[44] B. Dan, G. C. Irvin, M. Pasquali, *ACS Nano* **2009**, *3*, 835.
[45] B. B. Parekh, G. Fanchini, G. Eda, M. Chhowalla, *Appl. Phys. Lett.* **2007**, *90*, 121913.
[46] J. W. Jo, J. W. Jung, J. U. Lee, W. H. Jo, *ACS Nano* **2010**, *4*, 5382.
[47] Y. Zhou, L. Hu, G. Gruner, *Appl. Phys. Lett.* **2006**, *88*, 123109.
[48] W.-B. Liu, S. Pei, J. Du, B. Liu, L. Gao, Y. Su, C. Liu, H.-M. Cheng, *Adv. Funct. Mater.* **2011**, *21*, 2330.
[49] Z. Wu, Z. Chen, X. Du, J. M. Logan, J. Sippel, M. Nikolou, K. Kamaras, J. R. Reynolds, D. B. Tanner, A. F. Hebard, A. G. Rinzler, *Science* **2004**, *305*, 1273.
[50] A. G. Nasibulin, A. Kaskela, K. Mustonen, A. S. Anisimov, V. Ruiz, S. Kivistoì∧, S. Rackauskas, M. Y. Timmermans, M. Pudas, B. Aitchison, M. Kauppinen, D. P. Brown, O. G. Okhotnikov, E. I. Kauppinen, *ACS Nano* **2011**, *5*, 3214.
[51] D. Azulai, T. Belenkova, H. Gilon, Z. Barkay, G. Markovich, *Nano Lett.* **2009**, *9*, 4246.
[52] S. De, T. M. Higgins, P. E. Lyons, E. M. Doherty, P. N. Nirmalraj, W. J. Blau, J. J. Boland, J. N. Coleman, *ACS Nano* **2009**, *3*, 1767.